Multi band square-shaped polarization-insensitive graphene-based perfect absorber

Soheil Hadipour[1] · Pejman Rezaei[1] · Amirhossein Norouzi-Razani[2]

Abstract

In this manuscript, an original graphene-based metamaterial perfect absorber (MPA) was suggested and investigated with substituting aluminum with graphene. The proposed structure consists of a gold substrate as a conductive layer, a silicon substrate as a middle insulated layer and the patterned graphene layer as a resonator. The suggested structure, with only one metamaterial layer, has a lot of advantages such as simple implementation, cost-effectiveness, simple design and frequency tunability. The results of the proposed absorber, demonstrate that the absorber can provide absorption close to 100% at the frequencies of 0.56, 0.79, 1.02 and 1.25 THz by 0.9 eV graphene chemical potential (μc). With increasing the thickness of the silicone insulating layer, the absorption peaks number can be increased up to XIII bands. Also, changing the Fermi level can cause an absorption frequency shift. Furthermore, this structure is polarization insensitive and it is tolerating incident angles up to 45°. The recommended absorber is an appropriate candidate for filtering, spectroscopy, imaging and sensing application.

1 Introduction

Terahertz (THz) multiband absorbers have garnered significant consideration in latest years caused by their pivotal role in various industries such as medical, chemical and electrical engineering branch (Norouzi and Rezaei 2022a; Asl and Khajenoori 2021), ranging from telecommunications (Ye et al. 2022) and medical imaging (D'Arco et al. 2020) to security screening (Tribe et al. 2004) and spectroscopy (Yang et al. 2021). The terahertz region of the electromagnetics frequency range spanning approximately 100 GHz–10 THz (Kim et al. 2016), offers unique opportunities for material interaction and characterization. However, harnessing these capabilities requires efficient control over THz radiation, which is where multiband absorbers come into play (Khani and Hayati 2021).

✉ Pejman Rezaei
   prezaei@semnan.ac.ir

1   Electrical and Computer Engineering Faculty, Semnan University, Semnan, Iran

2   Department of Electrical Engineering, Amirkabir University of Technology, Tehran, Iran

At first a Russian physicist, Victor Veselago, presented metamaterials in 1968. These materials are artificial characterized by engineered structures and exhibit electromagnetic specifications that are not exist in natural material for example negative permittivity's imaginary part, negative refractive index and so on (Varshney and Giri 2021; Khani and Hayati 2022; Kiani et al. 2021). Metamaterials can be divided into several categories, graphene is one of these engineered structures which is two-dimensional with unique properties (Abohmra et al. 2022), a metamaterial that is consists of breaking graphite bonds which are demonstrated in Fig. 1. The unique properties of graphene such as small size and it is adjustable chemical potential that affects the graphene conductivity (Wang et al. 2016), cause use them in manufacture antenna (Failed 2023) to reduce the structure size and increase the antennas gain with controllable polarization (Chashmi et al. 2020), the design of resonators, electromagnetic shields, cloaking (Zhang et al. 2023; Zhimin et al. 2023), sensors (Norouzi Razani et al. 2022; Alipour et al. 2023; Kiani et al. 2020) and absorbers to inhibit the reflection or transmission.

Terahertz metamaterial absorbers, by controlling the graphene chemical potential with the bias voltage (external) specifically designed to achieve high absorption efficiency (near to 100%) and absorption bandwidth over specific frequency ranges, have attracted attention for their ability to surpass the limitations of conventional materials (Ghods and Rezaei 2018; Zhang et al. 2022). Conventional absorbers designed for single-frequency operation fall short when confronted with the complexity and diversity of modern THz applications. This ability to manipulate and absorb distinct frequencies opens up avenues for enhanced signal processing, improved imaging resolution and enhanced security protocols (Zamzam and Rezaei 2021; Khodadadi et al. 2022; Zamzam et al. 2023a; Kim and Hopwood 2019).

In absorbers, high absorption and polarization insensitivity are two important parameters (Zamzam et al. 2021). These features can cause absorber flexibility to be used in different applications such as Modulators (Emami-Nejad and Mir 2017), solar cells (Failed 2022; Sahin and Kabacelik 2018; Tang et al. 2016) and sensors for example Li et al(2021) designed early-stage cervical cancer identification with dual band terahertz metamaterial biosensor (Li et al. 2021).

Since graphene offers several advantages compared to aluminum when used in terahertz (THz) absorbers such as tunable absorption (Norouzi and Rezaei 2022b), ultra-thin material, compatibility with nanofabrication and environmental stability (Yong Zhang and He 2021) so, in this article, a multiband perfect metamaterial absorber (PMA) (Feng et al. 2020) is suggested by using Dongxia et al.'s article design and substitute graphene as a structure material with aluminum. At first simulations outcomes demonstrate the
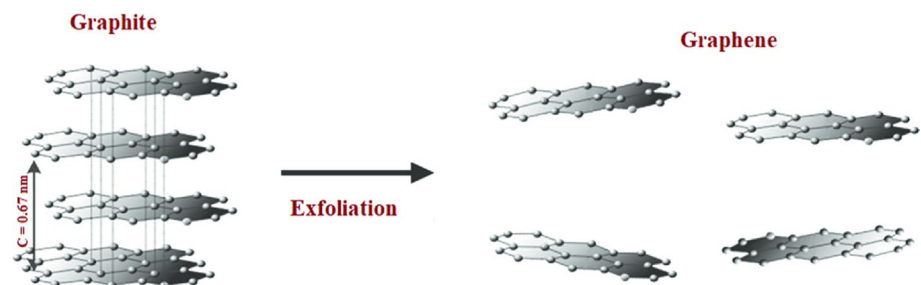

Fig. 1 Graphite exfoliation in order to create graphene

improvement of the suggested model to achieve the absorptivity rate of more than 90% in four picks of 0.56, 0.79, 1.02 and 1.25 THz. The multiband presented absorber is made of only one graphene layer, in comparison with multi-layer metamaterial, this feature of our suggested structure makes it easier to manufacture and inexpensive. This absorber consists of a square-shaped graphene surface layer, a silicon as an insulated spacer, along with the golden ground layer. From the simulation results, it can be obtained that, the suggested structure is very proper for sensing, imaging and other applications (Khodadadi et al. 2023a; Al-Ibadi 2022; Zamzam et al. 2023b; Nickpay et al. 2022).

2 Theoretical discussions and structure design

2.1 Theoretical discussions

The absorption ability of a metamaterial absorber (A) is calculated by the general absorption equation which is mentioned below (Zhong et al. 2020):

$$A = 1 - T - R \tag{1}$$

In this equation T is transmissivity and R is reflectivity. As expressed before, graphene is a two-dimensional controllable metamaterial, the graphenes' surface conductivity controlled with external gating which has tolerance from -1 to 1 eV and it can also be obtained from the Kubo formula which is indicated as follows (Khodadadi et al. 2023b; Hanson 2008):

$$\sigma_{intra}(\omega, E_F, \tau, T) = \sigma_{intra}(\omega, E_F, \tau, T) + \sigma_{inter}(\omega, E_F, \tau, T)\sigma_{intra} \tag{2}$$

$$\sigma_{intra}(\omega, E_F, \tau, T) = \frac{2k_B e^2 T}{\pi h^2} \ln\left[2\cosh\left(\frac{E_f}{2k_B T}\right)\right] \frac{i}{\omega + i\tau^{-1}} \tag{3}$$

$$\sigma_{inter}(\omega, E_F, \tau, T) = \frac{e^2}{4\hbar}\left[H\left(\frac{\omega}{2}\right) + \frac{4iw}{\pi}\int_0^\infty \frac{H(\varepsilon) - H\left(\frac{\omega}{2}\right)}{(w^2 - 4e^2)}d\varepsilon\right] \tag{4}$$

$$H(w) = \sinh\left[\hbar\varepsilon/(K_b T)\right] / \left\{\cosh\left[\frac{E_f}{K_b T}\right] + \cosh[\hbar\varepsilon/(K_b T)]\right\} \tag{5}$$

where ω, σ, τ, μ_c, E_F are the angular frequency, the graphene conductivity, the relaxation time of graphene, the graphene chemical potential and the Fermi energy value, respectively. In addition, e is the charge of electron with 1.6×10^{-19} c value, T = 300 K, h = the constant of reduced Plank's and K_b = the constant of Boltzmann. It is noticeable that according to the Pauli Exclusion Principle, in terahertz frequency band, we will have $E_F \gg K_b T$ so the inter-band part of the above formula becomes negligible. Consequently, the graphene conductivity equation will be simplified as the Drude model follow (Huang et al. 2018a):

$$\sigma\left(\omega, E_F, \tau, T\right) = \frac{e^2 E_f}{\pi h^2} \frac{i}{\omega + i\tau^{-1}} \tag{6}$$

As mentioned before the graphene's relaxation time can be obtained by Eq. (4)

$$\tau = \frac{\mu \mu_c}{eV_F^2} \tag{7}$$

where V_F and μ are the Fermi velocity with an approximately constant of 10^6m/s and the electron mobility.

2.2 Absorber structure design

The unit cell's geometrical structure is presented in Fig. 2, like most absorber structures, the presented absorber in this paper contains 3 layers. From upper to lowest layer, the absorber consists of a 0.01-µm thick graphene array on a middle layer of 190-µm thick high-resistance silicon as a dielectric or spacer layer with a constant of $\varepsilon = 11.9$. To avoid transmission to the other side of the metamaterial both of these layers are located on the gold as the third layer with a thickness of 0.5 µm and conductivity of $\sigma_{gold} = 4.56 \times 10^7$. The most effective dielectric with high capacitance is an ion-gel, it can be compatible with tunable graphene plasmonic devices on various substrates by its good mechanical flexibility and thermal stability, the structure diagram of the ion-gel top gate which can be used to control the Fermi energy of graphene is shown in Fig. 2d. After patterning an array of graphene we cover it with the ion-gel layer, which induces carrier concentration and allows
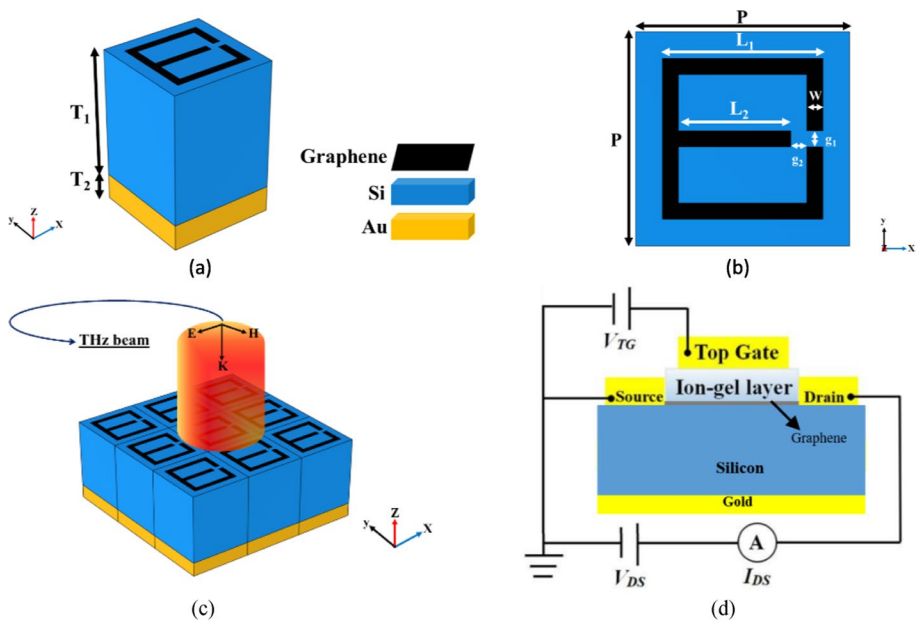

Fig. 2 Schematic of the suggested structure. **a** Side view of unit cell, **b** top view of unit cell, **c** absorber arrangement under terahertz beam radiation, **d** a layer of ion-gel which added to biasing the graphene
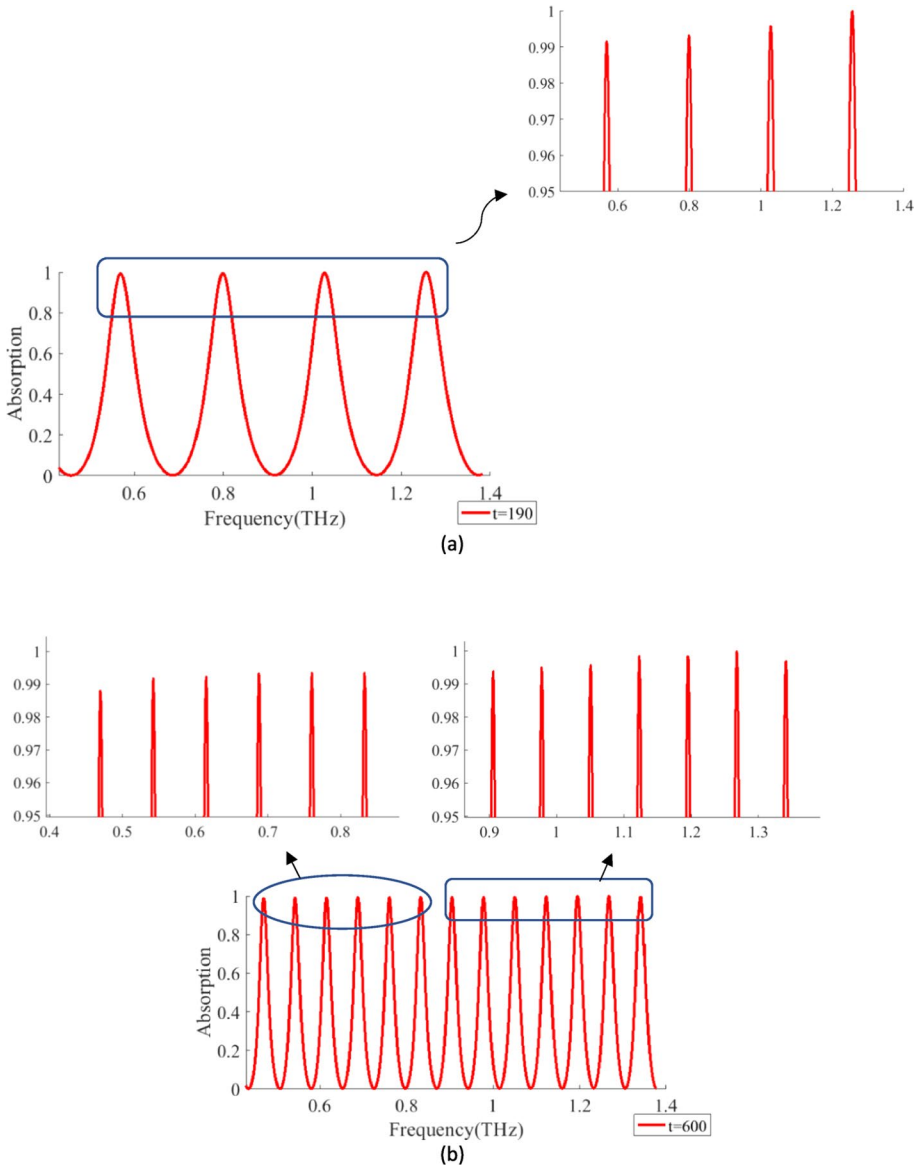
Fig. 3 Absorbance spectrum of the planned absorber for various Si layer thickness **a** 190 µm, **b** 600 µm

Table 1 The obtained values of the planned unit-cell (per µm)

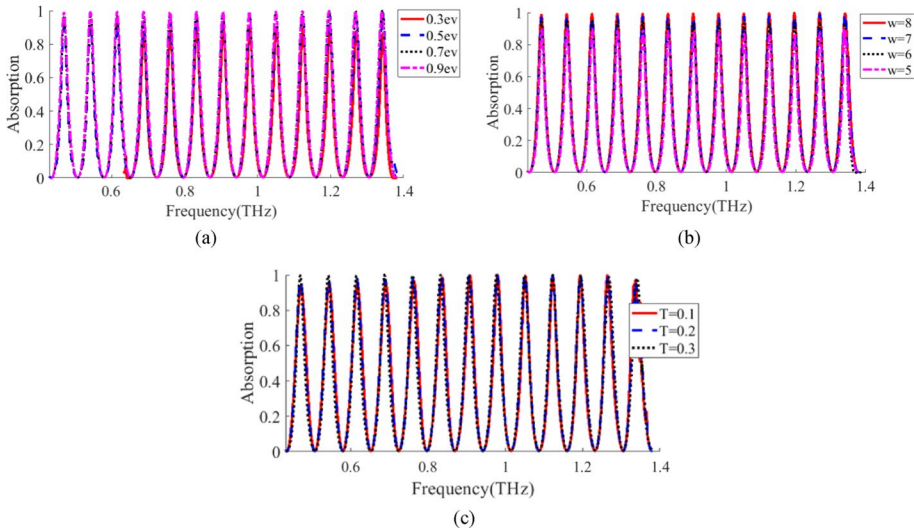| Dimension	Value	Dimension	Value
g_1	8	P	66
g_2	8	L_1	62
w	8	L_2	38

Fig. 4 The planned absorber absorption spectrum for various **a** graphene fermi-level, **b** graphene line width, **c** graphene relaxation time

the absorber to enter the terahertz band, we can give a conclusion ion-gel has little effect on the simulation results and we omit ion-gel to simplify the calculation.

One part of the incident light interacts with the graphene. The remained part passes through the graphene to reach the gold surface, which is reflected back by the gold and then lost in the silicon, to get a strong absorption mechanism, the imaginary parts of the relative permeability and/or permittivity can provide high magnetic and/or electrical losses for traveling waves absorption, so, by using a gold layer for the base layer of the structure, the transmission coefficient of the EM wave was decreased [$T(\omega) \to 0$].

The noticeable point is that to decrease the coefficient of the transmission (T) to zero, the base conductor layer thickness would be more than the THz range typical skin depth, so the absorption equation simplified to Eq. (8):

$$A = 1 - R \tag{8}$$

In our simulation, μ_c and τ were considered as 0.9 eV and 0.1 ps respectively, to get the optimum value We checked the various values of parameters and selected the best of them in the below table.

3 Simulation result and comparison

3.1 Simulation result

At first glance a quad-band absorber was designed as demonstrated in Fig. 3a with the same geometrical as mentioned in Table 1 and a thickness of 190 μm. Then by increasing the thick value to 600 μm absorption peak growth to XIII- band, so in this way the
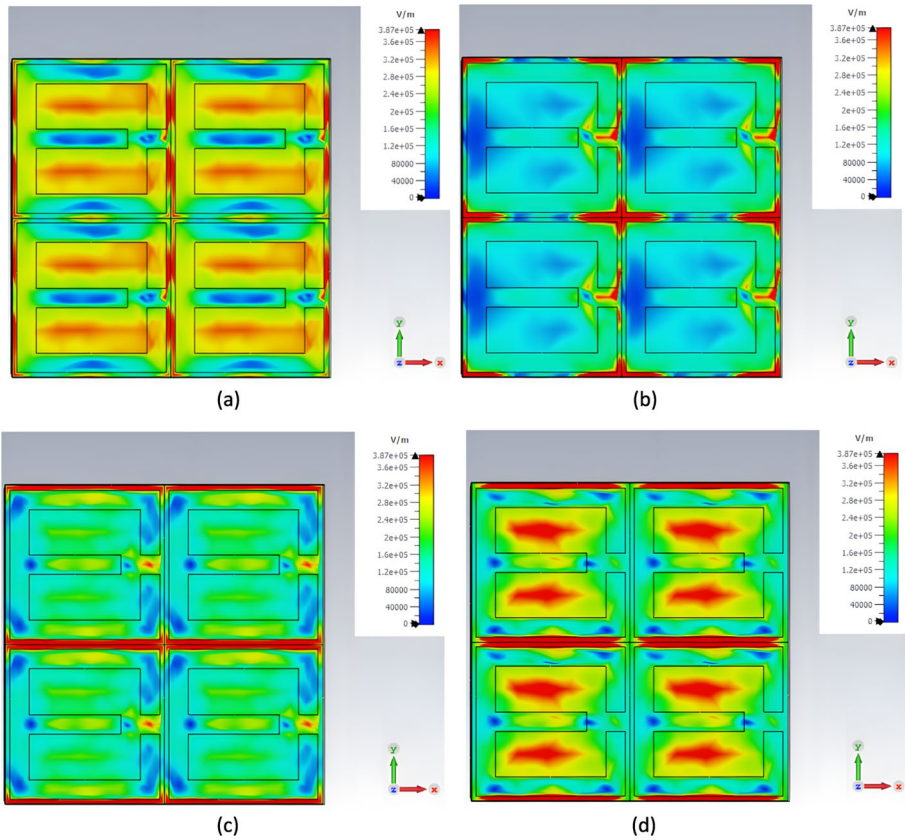
Fig. 5 Electrical field distribution of TE waves at **a** 0.49 THz, **b** 0.76 THz, **c** 1.05 THz, **d** 1.34 THz

absorption peaks number is controllable with dielectric thickness changing and the claim to reach XIII-band absorber become true. Figure 3b illustrates the absorbance spectrum of the suggested absorber and it is zoom figures. All the simulation was implemented in CST software based on the full-wave finite-integration-technique (FIT) at normal room temperature (300 K) and the accuracy of mesh in the graphene layer are set to 93.33 and 0.1 nm tetrahedrons mesh type, in addition the boundary condition considered as z_{max} open (add space), z_{min} electric (Et = 0).

Figure 4 simulation results, shows various value of (w), the graphene chemical potential and relaxation time to get the optimum result. As illustrated, only by substituting aluminum with graphene and a little change in the in-line width of the structure, both of absorption peak and average absorptivity increase. Four absorption peaks and more than 99.6% for average absorptivity. By using graphene, the claim that the proposed structure is tunable becomes true because changing the graphene fermi level (μc) can shift the absorption frequency without remanufacturing and even parameters changing. The maximum absorption
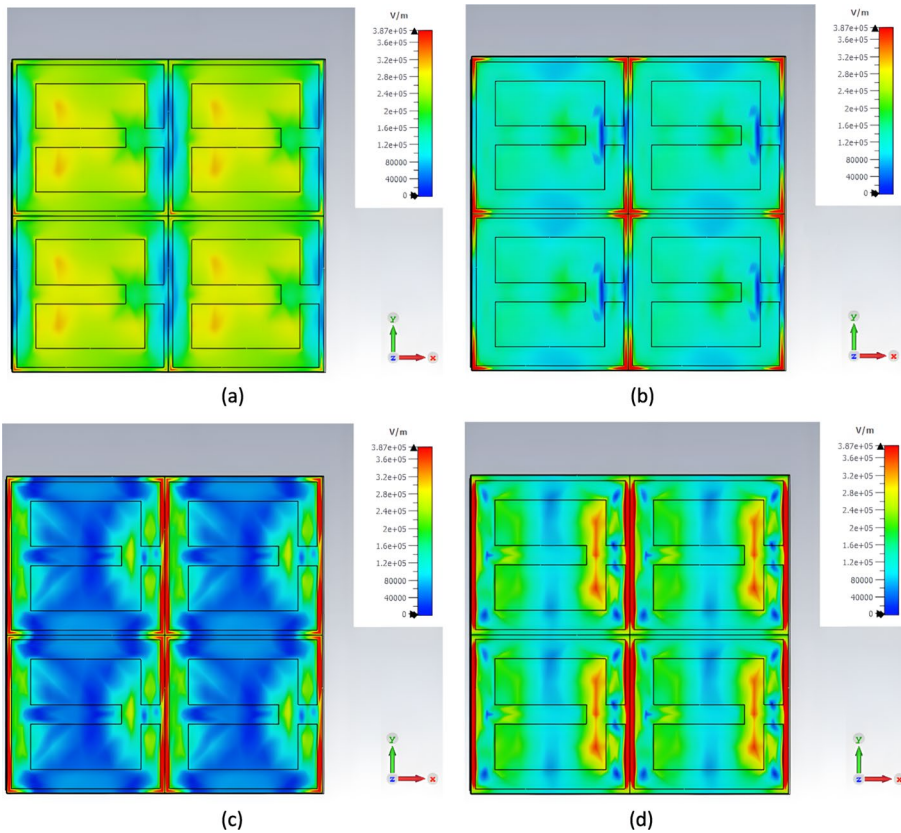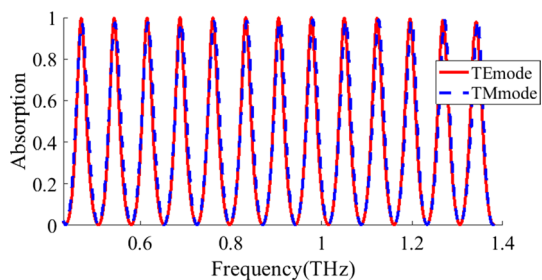
Fig. 6 Electrical field distributions of TM waves at **a** 0.49 THz, **b** 0.76 THz, **c** 1.05 THz, **d** 1.34 THz

Fig. 7 TE and TM mode of excitation

peaks resulted by μ_c =0.9 eV in Figs. 4a and 8 for graphene line width in Fig. 4b also τ = 0.1 ps is considered as the optimum value of graphene relaxation time in Fig. 4c.

Most multiband absorbers are challenging to fabricate because they make use of over one layer of metamaterials in their form or have a complicated construct although they're single layers. However, the presented structure uses only single layer of metamaterial in its construction and has an elementary plan. Therefore, they are completely lot simpler to fabricate than lookalike multiband structures.
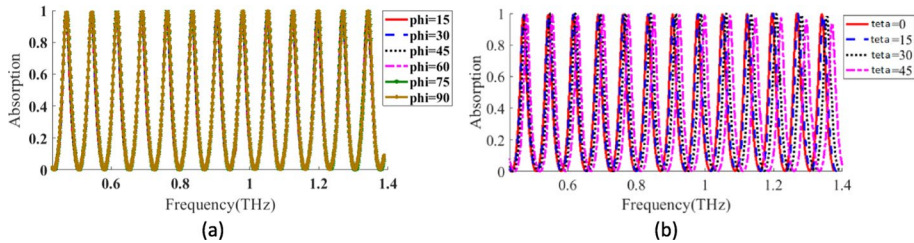
Fig. 8 The absorption spectrum for **a** insensitivity of polarization, **b** changes of incident angle

To describe the proposed absorber absorption mechanism, we mention the gold bottom layer considered as a ground layer which does not permit the radiated wave to pass through the arrangement. Furthermore, a silicon mid layer and a designed graphene layer located on top, neutralize the reflected waves by their phase difference, as a result perfect absorber seems reasonable.

Figure 5 displays the electrical field distribution in a normal incidence for TE modes. Similarly, Fig. 6 displays the electrical field distributions of TM modes briefly.

Here to compare the plot in both mode of excitation we show the figure of absorption where TE and TM mode of excitation plotted in a figure, so as shown in Fig. 7 TE and TM mode of excitation shows negligible differences on absorption peak.

3.1.1 Stability analysis

In this section, the angular and polarization stability of suggested absorber is considered by exposure to terahertz radiation along the 'z' axis. For evaluating the stability of polarization, TM and TE propagation modes are applied by increasing ϕ angle to 90° when the incidence angle (θ) is 0°. Even though, the suggested terahertz absorber is not in rotational form however Fig. 8a shows that the TM and TE modes are similar so, it's obvious that the absorption is stabile for both TM- and TE-modes therefore the claim that the presented absorbers are polarization insensitive become true. Moreover, Fig. 8b illustrates the study of how electromagnetic waves with a different angle of incidence affect their ability to be absorbed.

We evaluate the level of angular stability by looking at the range of angles, called θ, where the built absorber appears to have similar properties. So, the suggested terahertz absorber works well at any angle up to 45°. The terahertz absorber we showed works the same for different polarizations, so the way it behaves when the waves come at an angle is similar for both types of waves. Therefore, the planned absorber is stable when it comes to changes in angles and polarization.

Table 2 tries to compare this paper with reported results of other research from the standpoint of the peak numbers, average absorption, incident angle and polarization insensitive. It is obvious that in addition to polarization insensitivity the average absorption of absorber reached 99.60% in XIII bands which in comparison with other results in the table, it is slightly better.

In Table 2 the multiband absorber presented in this paper is compared with some other similar structures that were reported recently. Our final structure has the benefits of simple design, polarization insensitivity and high incident angle tolerance with

Table 2 The comparison of suggested absorber with similar reported work

References	Frequency (THz)	Peak numbers	Absorption average (%)	Incident angle	Polarization insensitive	Year
Li and Cheng (2020)	0.114, 0.181	2	98.95	0–45	Yes	2020
Huang et al. (2018b)	0.85, 3.37	2	95.15	0–80	Yes	2018
Veeraselvam and Mohammed (2021)	0.33, 0.90, 1.42, 1.85	4	99	0–60	Yes	2021
Hadipour and Rezaei (2023)	0.865, 1.43, 2	3	99.58	0–45	Yes	2023
Qin et al. (2020)	147, 188, 269	3	98.53	Normal	No	2020
Verma et al. (2019)	0.63, 1.55, 1.89, 2.33, 2.65, 2.91, 3.22, 3.42	8	93.99	0–90	Yes	2019
Huang et al. (2018)	1.6, 4.42, 4.94	3	99.06	0–60	Yes	2018
Mohanty et al. (2018)	1.45, 1.80, 2.70, 3.1, 3.7	5	80.24	0–90	Yes	2018
Yi (2019)	7.75, 14.85, 23.43	3	99	–	Yes	2019
Yuan et al. (2020)	0.94, 1.56	2	99.23	0–50	Yes	2020
Fan (2019)	469, 497.5	2	99.25	0–75	Yes	2019
Xiang et al. (2019)	22.33, 27.59	2	98.77	0–90	Yes	2019
Khatami et al. (2022)	2.7, 3.2, 3.99, 4.6	4	99.43	0–60	Yes	2022
Wang et al. (2020)	1.59, 2.45, 3.05, 4.41, 5.11	5	97.35	–	–	2020
Proposed	0.49, 0.65, 0.79, 094, ….,	XIII	99.60	0–45	Yes	2023

the desired absorption peak with average absorption of 99.60%. All the characteristics make the final structure very flexible and a good candidate for sensing, imaging, spectroscopy and some other absorbing application.

4 Conclusion

In this paper, at first, a dual-band THz absorber based on aluminum was designed for sensor application to diagnose early-stage cervical cancer. Because of graphene's several advantages compared to aluminum by substituting the surface material of the sensor with graphene and adding a gold ground layer our proposed model formed. In comprehension between the new suggested absorber and the previous model, two absorption peaks were added and overall absorptivity was increased. We investigated an multi band tunable metamaterial structure that is polarization insensitive and tolerates incident angles up to 45°, in addition to all these features the flexibility and high absorbance characteristics, make it a candidate for our proposed model for filtering, imaging, sensing and other applications.

Data availability All data generated or analyzed during this study are included in this published article.

Declarations

Conflict of interest The authors declare that they have no conflict of interest.

Ethical approval We declare that this article is original, has not been published before and is not currently considered for publication elsewhere. We confirm that the manuscript has been read and approved by all named authors and that there are no other persons who satisfied the criteria for authorship but are not listed. We further confirm that the order of authors listed in the manuscript has been approved by all of us.

Consent to participate Written informed consent for participation was obtained from all participants.

References

Abohmra, A., Khan, Z.U., Abbas, H.T., Shoaib, N.: Two-dimensional materials for future terahertz wireless communications. IEEE Open J. Antennas Propag. **3**, 217–228 (2022)

Al-Ibadi, A.: Ex vivo terahertz imaging reflection of malignant and benign human breast tumors. Malas. J. Sci. **41**, 17–22 (2022)

Alipour, A.H., et al.: Trapped multimodal resonance in magnetic field enhancement and sensitive THz plasmon sensor for toxic materials accusation. IEEE Sens. J. **23**(13), 14057–14066 (2023)

An, Z., Huang, Y., Zhang, R.: High-temperature multispectral stealth metastructure from the microwave-infrared compatible design. Compos. B Eng. **259**, 110737 (2023)

Asl, A.H., Khajenoori, M.: Green Extraction in Separation Technology. CRC Press, Boca Raton (2021)

Chashmi, M.J., Rezaei, P., Kiani, N.: Y-shaped graphene-based antenna with switchable circular polarization. Optik **200**, 163321 (2020)

D'Arco, A., Di Fabrizio, M., Dolci, V., Petrarca, M., Lupi, S.: THz pulsed imaging in biomedical applications. Condens. Matter **5**, 1–28 (2020)

Emami-Nejad, H., Mir, A.: Design and simulation of a flexible and ultrasensitive biosensor based on frequency selective surface in the microwave range. Opt. Quantum Electron. **49**(10), 1–15 (2017)

Fan, Y.: Dual-band perfect light absorber in visible region based on cylinder silicon resonator. Optik **179**, 1084–1090 (2019)

Feng, Y., Hu, Z.D., Balmakou, A., Khakhomov, S.: Perfect narrowband absorber based on patterned graphene-silica multilayer hyperbolic metamaterials. Plasmonics **15**, 1869–1874 (2020)

Ghods, M.M., Rezaei, P.: Ultra-wideband microwave absorber based on uncharged graphene layers. J. Electromagn. Waves Appl. **32**(15), 1950–1960 (2018)

Hadipour, S., Rezaei, P.: A graphene-based triple-band THz metamaterial absorber for cancer early detection. Opt. Quantum Electron. **55**(13), 1122 (2023)

Hanson, G.: Dyadic green's functions for an anisotropic, non-local model of biased graphene. IEEE Trans. Antennas Propag. **56**(3), 747–757 (2008)

Huang, X., et al.: Multiband ultrathin polarization insensitive terahertz perfect absorbers with complementary metamaterial and resonator based on high-order electric and magnetic resonances. IEEE Photon. J. **10**(6), 1–11 (2018)

Huang, M., Cheng, Y., Cheng, Z., Chen, H., Mao, X., Gong, R.: Based on graphene tunable dual-band terahertz metamaterial absorber with wide-angle. Opt. Commun. **415**, 194–201 (2018a)

Khani, S., Hayati, M.: An ultra-high sensitive plasmonic refractive index sensor using an elliptical resonator and MIM waveguide. Superlattices Microstruct. **56**, 106970 (2021)

Khani, S., Hayati, M.: Optical biosensors using plasmonic and photonic crystal band-gap structures for the detection of basal cell cancer. Sci. Rep. **12**(1), 5246 (2022)

Khatami, S.A., Rezaei, P., Zamzam, P.: Quad band metal-dielectric-metal perfect absorber to selective sensing application. Opt. Quantum Electron. **54**, 638 (2022)

Khodadadi, B., et al.: Wideband polarization-insensitive metamaterial perfect absorber based on bilayer graphene metasurface. Opt. Quantum Electron. **54**(11), 734 (2022)

Khodadadi, B., et al.: Sensitivity increment of metamaterial-based refractive index sensor with silicon layers. SILICON **15**, 6745–6759 (2023a)

Khodadadi, B., et al.: Triple-band metamaterial perfect absorber for refractive index sensing in THz frequency. Opt. Quantum Electron. **431**, 55 (2023b)

Kiani, S., Rezaei, P., Navaei, M.: Dual-sensing and dual-frequency microwave SRR sensor for liquid samples permittivity detection. Measurement **160**, 107805 (2020)

Kiani, S., Rezaei, P., Fakhr, M.: Dual-frequency microwave resonant sensor to detect non-invasive glucose level changes through the fingertip. IEEE Trans. Instrum. Meas. **70**, 1–8 (2021)

Kiani, N., et al.: Designing of a circularly polarized reconfigurable graphene-based THz patch antenna with cross-shaped slot. Opt. Quantum Electron. **55**, 356 (2023)

Kim, H., Hopwood, J.: Wave propagation in composites of plasma and metamaterials with negative permittivity and permeability. Sci. Rep. **9**, 3024 (2019)

Kim, J.H., Hokmabadi, M.P., Balci, S., Rivera, E., Wilbert, D.: Investigation of robust flexible conformal THz perfect metamaterial absorber. Appl. Phys. A **122**, 362 (2016)

Li, W., Cheng, Y.: Dual-band tunable terahertz perfect metamaterial absorber based on strontium titanate (STO) resonator structure. Opt. Commun. **462**, 125265 (2020)

Li, D., et al.: Identification of early-stage cervical cancer tissue using metamaterial terahertz biosensor with two resonant absorption frequencies. IEEE J. Sel. Top. Quantum Electron. **27**, 1–7 (2021)

Mohanty, A., Acharya, O.P., Appasani, B., Mohapatra, S.K.: A multi-band terahertz metamaterial absorber based on a Π and U-shaped structure. Photon. Nanostruct. **32**, 74–80 (2018)

Nickpay, M.R., Danaie, M., Shahzadi, A.: Design of a graphene-based multi-band metamaterial perfect absorber in THz frequency region for refractive index sensing. Phys. E **138**, 115114 (2022)

Norouzi, A., Rezaei, P.: Multiband polarization insensitive and tunable terahertz metamaterial perfect absorber based on the heterogeneous structure of graphene. Opt. Quantum Electron. **54**, 407 (2022a)

Norouzi, A., Rezaei, P.: Broadband polarization insensitive and tunable terahertz metamaterial perfect absorber based on the graphene disk and square ribbon. Micro Nanostruct. **163**, 107153 (2022b)

Qin, F., et al.: A tunable triple-band near-infrared metamaterial absorber based on Au nanocuboids array. Nanomaterials **10**(2), 207 (2020)

Razani, A.N., et al.: Absorption-based ultra-sensitive RI sensor based on the flower-shaped graphene resonator for early detection of cancer. Opt. Commun. **524**, 128775 (2022)

Sahin, R., Kabacelik, I.: Effects of ionizing radiation on the properties of mono-crystalline Si solar cells. Radiat. Phys. Chem. **150**, 90–94 (2018)

Tang, J., Xiao, Z., Xu, K.: Ultra-thin metamaterial absorber with extremely bandwidth for solar cell and sensing applications in visible. Opt. Mater. **60**, 142–147 (2016)

Tribe, W.R., Newnham, D.A., Taday, P.F.: Hidden object detection: security applications of terahertz technology. Proc. SPIE **5354**, 168–176 (2004)

Varshney, G., Giri, P.: Bipolar charge trapping for absorption enhancement in a graphene-based ultrathin dual-band terahertz biosensor. Nanoscale Adv. **3**, 5813–5822 (2021)

Veeraselvam, A., Mohammed, G.: A novel multi-band biomedical sensor for THz regime. Opt. Quantum Electron. **53**, 354 (2021)

Verma, V.K., Mishra, S.K., Kaushal, K.K.: An octaband polarization insensitive terahertz metamaterial absorber using orthogonal elliptical ring resonators. Plasmonics **15**, 75–81 (2019)

Wang, T., et al.: Experimental realization of perfect terahertz plasmonic absorbers using highly doped silicon substrate and COMS-compatible techniques. Opt. Mater. Express **6**, 523–530 (2016)

Wang, B.X., He, Y., Lou, P., Huang, W.Q., Pi, F.: Penta-band terahertz light absorber using five localized resonance responses of three patterned resonators. Results Phys. **16**, 102930 (2020)

Xiang, Y., Wang, L., Lin, Q., Xia, S., Qin, M., Zhai, X.: Tunable dual-band perfect absorber based on L-shaped graphene resonator. IEEE Photon. Technol. Lett. **31**, 483–486 (2019)

Yang, S., Du, C., Feng, L., Zhang, C., Wu, J.: Real-time near-field terahertz spectroscopy imaging. In: 46th International Conference on Infrared, Millimeter and Terahertz Waves, Chengdu, China, p. 1 (2021)

Yao, H., et al.: Patterned graphene and terahertz metasurface-enabled multidimensional ultra-sensitive flexible biosensors and bio-assisted optical modulation. Results Phys. **40**, 105884 (2022)

Ye, J., Dang, S., Ma, G., Amin, O., Shihada, B., Alouini, M.S.: On outage performance of terahertz wireless communication systems. IEEE Trans. Commun. **70**, 649–663 (2022)

Yi, Z., et al.: Graphene-based tunable triple-band plasmonic perfect metamaterial absorber with good angle-polarization-tolerance. Results Phys. **13**, 102149 (2019)

Yuan, S., Yang, R., Tian, J., Zhang, W.: A photoexcited switchable tristate terahertz metamaterial absorber. Int. J. RF Microw. Comput. Aided Eng. **30**(1), e22014 (2020)

Zamzam, P., Rezaei, P.: A terahertz dual-band metamaterial perfect absorber based on metal-dielectric-metal multi-layer columns. Opt. Quantum Electron. **53**(2), 109 (2021)

Zamzam, P., Rezaei, P., Khatami, S.A.: Quad-band polarization-insensitive metamaterial perfect absorber based on bilayer graphene metasurface. Phys. E **128**, 114621 (2021)

Zamzam, P., et al.: Band reduplication of perfect metamaterial terahertz absorber with an added layer: cross symmetry concept. Opt. Quantum Electron. **55**, 391 (2023a)

Zamzam, P., et al.: Graphene-based polarization-insensitive metamaterials with perfect absorption for terahertz biosensing applications: analytical approach. Opt. Laser Technol. **163**, 109444 (2023b)

Zhang, Y., He, Y., Wang, H., Sun, L., Su, Y.: Ultra-broadband mode size converter using on-chip metamaterial-based Luneburg lens. ACS Photon. **8**(1), 202–208 (2021)

Zhang, H., Zeng, B., Gao, E., Yao, P., Liu, C., Li, H.: Dynamically tunable terahertz sensors based on dual-layered graphene metamaterial. Opt. Commun. **506**, 127555 (2022)

Zhang, Y., et al.: Functional additive manufacturing of large-size metastructure with efficient electromagnetic absorption and mechanical adaptation. Compos. Part A Appl. Sci. Manuf. **173**, 107652 (2023)

Zhong, Q., Wang, T., Jiang, X., Cheng, L., Yan, R.: Near-infrared multi narrowband absorber based on plasmonic nanopillar metamaterial. Opt. Commun. **458**, 124637 (2020)